

# Implications of 3+1 Short-Baseline Neutrino Oscillations

Carlo Giunti\*

*INFN, Sezione di Torino, Via P. Giuria 1, I-10125 Torino, Italy*

Marco Laveder†

*Dipartimento di Fisica “G. Galilei”, Università di Padova, and INFN,  
Sezione di Padova, Via F. Marzolo 8, I-35131 Padova, Italy*

(Dated: November 23, 2011)

We present an upgrade of the 3+1 global fit of short-baseline neutrino oscillation data obtained with the addition of KARMEN and LSND  $\nu_e + {}^{12}\text{C} \rightarrow {}^{12}\text{N}_{\text{g.s.}} + e^-$  scattering data. We discuss the implications for the measurements of the effective neutrino mass in  $\beta$ -decay and neutrinoless double- $\beta$ -decay experiments. We find respective predicted ranges of about 0.1–0.7 eV and 0.01–0.1 eV.

PACS numbers: 14.60.Pq, 14.60.Lm, 14.60.St

## I. INTRODUCTION

The study of active-sterile neutrino oscillations received recently a boost from indications in favor of possible short-baseline oscillations of two types: 1)  $\bar{\nu}_\mu \rightarrow \bar{\nu}_e$  oscillations observed in the LSND [1] and MiniBooNE [2] experiments; 2)  $\bar{\nu}_e$  and  $\nu_e$  disappearance revealed, respectively, by the Reactor Anomaly [3] and the Gallium Anomaly [4–10]. In this paper we consider these indications in the framework of hierarchical 3+1 neutrino mixing and we discuss the implications for the measurements of the effective neutrino mass in  $\beta$ -decay and neutrinoless double- $\beta$ -decay experiments. We also upgrade the global fit presented in Ref. [11] by the addition of KARMEN [12, 13] and LSND [14]  $\nu_e + {}^{12}\text{C} \rightarrow {}^{12}\text{N}_{\text{g.s.}} + e^-$  scattering data, as suggested in Ref. [15].

Short-baseline (SBL) neutrino oscillations are generated by a squared-mass difference  $\Delta m_{\text{SBL}}^2 \gtrsim 0.1 \text{ eV}^2$ , which is much larger than the two measured solar (SOL) and atmospheric (ATM) squared-mass differences  $\Delta m_{\text{SOL}}^2 = (7.6 \pm 0.2) \times 10^{-5} \text{ eV}^2$  [16] and  $\Delta m_{\text{ATM}}^2 = 2.32^{+0.12}_{-0.08} \times 10^{-3} \text{ eV}^2$  [17]. The minimal neutrino mixing schemes which can provide a third squared-mass difference for short-baseline neutrino oscillations require the introduction of a sterile neutrino  $\nu_s$  (see Refs. [18–21]). Hierarchical 3+1 neutrino mixing is a perturbation of the standard three-neutrino mixing in which the three active neutrinos  $\nu_e, \nu_\mu, \nu_\tau$  are mainly composed of three massive neutrinos  $\nu_1, \nu_2, \nu_3$  with light masses  $m_1, m_2, m_3$ , such that  $\Delta m_{\text{SOL}}^2 = \Delta m_{21}^2$  and  $\Delta m_{\text{ATM}}^2 = |\Delta m_{31}^2| \simeq |\Delta m_{32}^2|$ , with the standard notation  $\Delta m_{kj}^2 \equiv m_k^2 - m_j^2$  (see Ref. [22]). The sterile neutrino is mainly composed of a heavy neutrino  $\nu_4$  with mass  $m_4$  such that  $\Delta m_{\text{SBL}}^2 = \Delta m_{41}^2$  and

$$m_1, m_2, m_3 \ll m_4 \quad \Rightarrow \quad m_4 \simeq \sqrt{\Delta m_{41}^2}. \quad (1)$$

Under these hypotheses, the effects of active-sterile neutrino mixing in solar [23, 24] and atmospheric [25–28] neutrino experiments are small, but should be revealed sooner or later.

In 3+1 neutrino mixing, the effective flavor transition and survival probabilities in short-baseline neutrino oscillation experiments are given by (see Refs. [18–21])

$$P_{\nu_\alpha \rightarrow \nu_\beta}^{\text{SBL}(-)} = \sin^2 2\vartheta_{\alpha\beta} \sin^2 \left( \frac{\Delta m_{41}^2 L}{4E} \right) \quad (\alpha \neq \beta), \quad (2)$$

$$P_{\nu_\alpha \rightarrow \nu_\alpha}^{\text{SBL}(-)} = 1 - \sin^2 2\vartheta_{\alpha\alpha} \sin^2 \left( \frac{\Delta m_{41}^2 L}{4E} \right), \quad (3)$$

for  $\alpha, \beta = e, \mu, \tau, s$ , with the transition amplitudes

$$\sin^2 2\vartheta_{\alpha\beta} = 4|U_{\alpha 4}|^2 |U_{\beta 4}|^2, \quad (4)$$

$$\sin^2 2\vartheta_{\alpha\alpha} = 4|U_{\alpha 4}|^2 (1 - |U_{\alpha 4}|^2). \quad (5)$$

The hierarchical 3+1 scheme may be compatible with the results of standard cosmological  $\Lambda$ CDM analyses of the Cosmic Microwave Background and Large-Scale Structures data, which constrain the three light neutrino masses to be much smaller than 1 eV [29–32] and indicate that one or two sterile neutrinos may have been thermalized in the early Universe [33–40], with an upper limit of the order of 1 eV on their masses. Also Big-Bang Nucleosynthesis data [41, 42] are compatible with the existence of sterile neutrinos, with the indication however that the thermalization of more than one sterile neutrino is disfavored [38, 43].

The global fit presented in this paper upgrades that presented in Ref. [11] by the addition of  $\nu_e + {}^{12}\text{C} \rightarrow {}^{12}\text{N}_{\text{g.s.}} + e^-$  scattering data, as suggested in Ref. [15]. The considered sets of data are:

- The short-baseline  $\bar{\nu}_\mu \rightarrow \bar{\nu}_e$  data of the LSND [1], KARMEN [45], NOMAD [46] and MiniBooNE neutrino [47] and antineutrino [2, 48, 49] experiments.
- The short-baseline  $\bar{\nu}_e$  disappearance data of the Bugey-3 [50], Bugey-4 [51], ROVNO91 [52], Gosgen

\* giunti@to.infn.it; also at Department of Theoretical Physics, University of Torino, Italy

† laveder@pd.infn.it

		REA	GAL	CAR	RGC	GLO-LOW	GLO-HIG
No Osc.	$\chi^2_{\min}$	27.1	12.0	8.2	47.3	195.1	178.1
	NDF	38	4	10	52	144	138
	GoF	0.91	0.017	0.61	0.66	0.0049	0.019
3+1	$\chi^2_{\min}$	21.7	2.3	4.6	36.2	152.4	137.5
	NDF	36	2	8	50	144	138
	GoF	97%	32%	80%	93%	30%	50%
	$\Delta m^2_{41} [\text{eV}^2]$	1.95	2.24	13.80	7.59	0.9	1.6
	$ U_{e4} ^2$	0.026	0.15	0.13	0.036	0.027	0.036
	$ U_{\mu 4} ^2$					0.021	0.0084
	$\sin^2 2\vartheta_{e\mu}$					0.0023	0.0012
	$\sin^2 2\vartheta_{ee}$	0.10	0.51	0.45	0.14	0.10	0.14
	$\sin^2 2\vartheta_{\mu\mu}$					0.083	0.034
PG	$\Delta\chi^2_{\min}$				7.6	18.8	11.6
	NDF				4	2	2
	GoF				11%	0.008%	0.3%

TABLE I. Values of  $\chi^2$ , number of degrees of freedom (NDF), goodness-of-fit (GoF) and best-fit values of the 3+1 oscillation parameters obtained from the fits of Gallium (GAL), Reactor (REA),  $\nu_e$ - $^{12}\text{C}$  (CAR) data, their combined fit (RGC) and the global fit with (GLO-LOW) and without (GLO-HIG) the MiniBooNE electron neutrino and antineutrino data with reconstructed neutrino energy smaller than 475 MeV. The first three lines correspond to the case of no oscillations (No Osc.). The following nine lines correspond to the case of 3+1 mixing. The last three lines give the parameter goodness-of-fit (PG) [44].

	REA+TRI	GAL+TRI	CAR+TRI	RGCT	GLO-LOW	GLO-HIG
$m_4$	1.3 – 5.2	1.0 – 2.8	2.7 – 3.8	1.4 – 3.8	0.91 – 2.5	1.2 – 2.4
	0.41 – 13	0.85 – 5.2	< 245	1.2 – 8.4	0.88 – 2.5	0.91 – 2.5
	< 343	0.22 – 11	< 412	0.42 – 16	0.85 – 2.8	0.87 – 2.8
$ U_{e4} ^2$	0.01 – 0.04	0.09 – 0.20	0.03 – 0.14	0.02 – 0.05	0.02 – 0.04	0.03 – 0.05
	0.00 – 0.05	0.04 – 0.28	–	0.01 – 0.06	0.02 – 0.06	0.02 – 0.06
	< 0.06	> 0.00	–	0.00 – 0.07	0.01 – 0.07	0.01 – 0.07
$m_{\beta}^{(4)}$	0.16 – 0.81	0.36 – 1.06	0.48 – 1.40	0.23 – 0.74	0.14 – 0.49	0.21 – 0.45
	0.02 – 1.69	0.23 – 1.79	< 1.79	0.15 – 1.45	0.12 – 0.56	0.13 – 0.56
	< 2.29	0.05 – 2.29	< 2.29	0.02 – 2.15	0.10 – 0.65	0.11 – 0.63
$m_{\beta\beta}^{(4)}$	0.021 – 0.13	0.110 – 0.41	0.081 – 0.51	0.039 – 0.15	0.020 – 0.10	0.035 – 0.09
	< 0.30	0.048 – 0.76	< 0.78	0.019 – 0.28	0.015 – 0.13	0.018 – 0.12
	< 0.42	0.003 – 1.03	< 1.17	0.001 – 0.44	0.011 – 0.16	0.013 – 0.16

TABLE II. Allowed  $1\sigma$ ,  $2\sigma$  and  $3\sigma$  ranges of  $m_4 = \sqrt{\Delta m^2_{41}}$ ,  $|U_{e4}|^2$ ,  $m_{\beta}^{(4)} = |U_{e4}| \sqrt{\Delta m^2_{41}}$  and  $m_{\beta\beta}^{(4)} = |U_{e4}|^2 \sqrt{\Delta m^2_{41}}$  obtained from the fits of Tritium data with Gallium (GAL+TRI), Reactor (REA+TRI) and  $\nu_e$ - $^{12}\text{C}$  (CAR+TRI) data, their combined fit (RGCT) and the global fit with (GLO-LOW) and without (GLO-HIG) the MiniBooNE electron neutrino and antineutrino data with reconstructed neutrino energy smaller than 475 MeV. Masses are given in eV.

[53], ILL [54] and Krasnoyarsk [55] reactor antineutrino experiments, taking into account the new calculation of the reactor  $\bar{\nu}_e$  flux [56, 57] which indicates a small  $\bar{\nu}_e$  disappearance (the reactor antineutrino anomaly [3]), and the KamLAND [58] bound on  $|U_{e4}|^2$  (see Ref. [59]).

- The short-baseline  $\nu_{\mu}$  disappearance data of the CDHSW experiment [60], the constraints on  $|U_{\mu 4}|^2$  obtained in Ref. [61] from the analysis of the data of atmospheric neutrino oscillation experiments, and the bound on  $|U_{\mu 4}|^2$  obtained from MINOS neutral-current data [62] (see Refs. [11, 63]).
- The data of Gallium radioactive source experiments (GALLEX [4–6] and SAGE [7–10]) which indicate a  $\nu_e$  disappearance (the Gallium neutrino anomaly

[3, 64–72]). We analyze the Gallium data according to Ref. [72].

- The  $\nu_e + ^{12}\text{C} \rightarrow ^{12}\text{N}_{\text{g.s.}} + e^-$  scattering data of the KARMEN [12, 13] and LSND [14] experiments, which constrain the short-baseline  $\nu_e$  disappearance [15].

The plan of the paper is as follows. Since this is the first time that the KARMEN and LSND  $\nu_e + ^{12}\text{C} \rightarrow ^{12}\text{N}_{\text{g.s.}} + e^-$  scattering data are taken into account in a global fit of neutrino oscillation short-baseline data, in Section II we discuss the method of the analysis and we present the ensuing upgrade of the global fit published in Ref. [11]. In Section III we discuss the predictions for the effective electron neutrino mass in  $\beta$ -decay. In Section IV we present the predictions for the effective

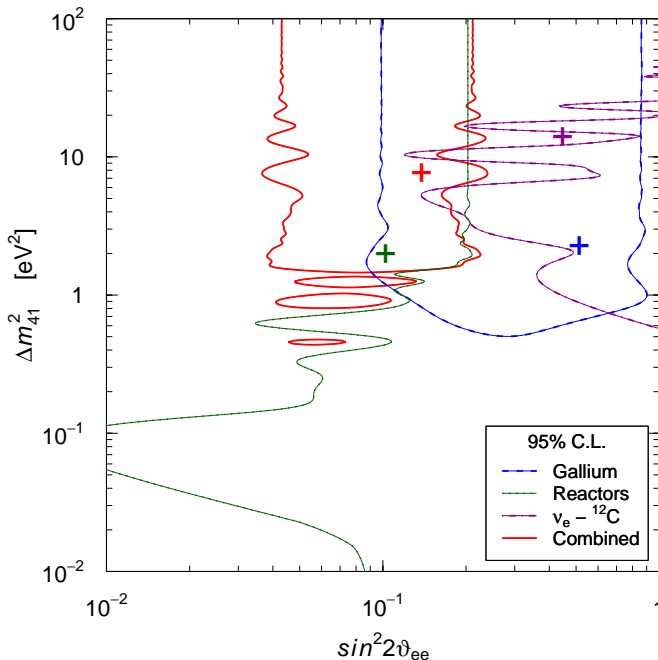


FIG. 1. Superposition of the 95% C.L. contours in the  $\sin^2 2\vartheta_{ee}-\Delta m_{41}^2$  plane obtained from the separate fits of Gallium, reactor and  $\nu_e - ^{12}\text{C}$  data and that obtained from the combined fit. The best-fit points are indicated by crosses (see Table. I).

Majorana neutrino mass in neutrinoless double- $\beta$ -decay. In Section V we draw our conclusions.

## II. GLOBAL FIT

In this section we present the upgrade of the results of the global fit of short-baseline neutrino oscillation data obtained in Ref. [11] with the inclusion of the KARMEN [12, 13] and LSND [14]  $\nu_e + ^{12}\text{C} \rightarrow ^{12}\text{N}_{\text{g.s.}} + e^-$  scattering data suggested in Ref. [15].

We analyzed the KARMEN and LSND data summarized in Ref. [15] without assuming a theoretical model for the  $\nu_e + ^{12}\text{C} \rightarrow ^{12}\text{N}_{\text{g.s.}} + e^-$  cross section. We assumed only a dependence of the cross section on  $(E-Q)^2$ , where  $Q = 17.3$  MeV is the  $Q$ -value of the reaction. Such dependence on the neutrino energy  $E$  is due to the allowed character of the transition from the  $0^+$  ground state of  $^{12}\text{C}$  to the  $1^+$  ground state of  $^{12}\text{N}$ . The information on neutrino oscillations comes from the different source-detector distances in KARMEN and LSND:  $L_{\text{KARMEN}} = 17.7$  m and  $L_{\text{LSND}} = 29.8$  m. The best fit values of the oscillation parameters and the 95% C.L. allowed region in the  $\sin^2 2\vartheta_{ee}-\Delta m_{41}^2$  plane are given, respectively, in Tab. I and Fig. 1, together with the corresponding quantities obtained from the analysis of reactor and Gallium data.

The  $\nu_e - ^{12}\text{C}$  curve in Fig. 1 is an exclusion curve which proscribes the region of the oscillation parameters on the

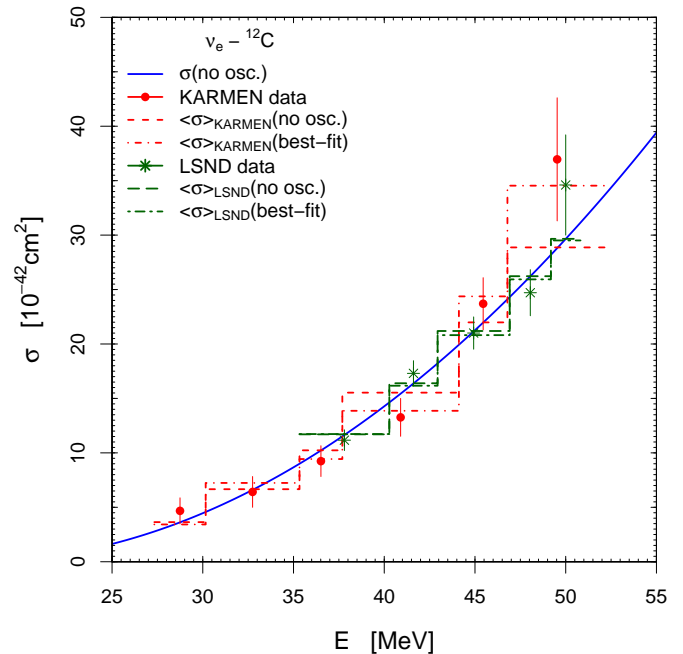


FIG. 2. KARMEN and LSND  $\nu_e - ^{12}\text{C}$  cross section data (points and asterisks, respectively) with the corresponding statistical error bars. The solid blue line shows the best-fit dependence of the cross section on the neutrino energy  $E$  in the case of no oscillations. The dashed red and long-dashed green histograms show, respectively, the corresponding average cross section for the energy bins of the KARMEN and LSND data. The dash-dotted red and long-dash-dotted green histograms show, respectively, the average cross section modulated by the best-fit oscillation probability for the energy bins of the KARMEN and LSND data.

right. The best-fit is obtained for rather large values of the oscillation parameters:  $\Delta m_{41}^2 = 13.80 \text{ eV}^2$  and  $\sin^2 2\vartheta_{ee} = 0.45$ . The reason of the improvement of the value of  $\chi_{\text{min}}^2$  obtained with the best-fit values of the oscillation parameters with respect to the case of no oscillations can be understood from Fig. 2, where one can see that there is an improvement in the fit of the KARMEN data due to the shorter source-detector distance with respect to the LSND data, for which there is practically no improvement, because oscillations are averaged out. From Fig. 1 one can see that for  $\Delta m_{41}^2 \gtrsim 20 \text{ eV}^2$  there is no constraint on neutrino oscillations from  $\nu_e - ^{12}\text{C}$  because the oscillations are averaged out in both the KARMEN and LSND experiments.

The comparison of the 95% C.L. reactor, Gallium and  $\nu_e - ^{12}\text{C}$  allowed regions in the  $\sin^2 2\vartheta_{ee}-\Delta m_{41}^2$  plane presented in Fig. 1 shows that there is a region of overlap for  $0.1 \lesssim \sin^2 2\vartheta_{ee} \lesssim 0.2$  and  $\Delta m_{41}^2 \gtrsim 2 \text{ eV}^2$ , indicating that the results of the three sets of data are compatible with the hypothesis of neutrino oscillations.

Figure 1 shows also the 95% C.L. allowed region in the  $\sin^2 2\vartheta_{ee}-\Delta m_{41}^2$  plane obtained from the combined analysis of reactor, Gallium and  $\nu_e - ^{12}\text{C}$ , with the best-

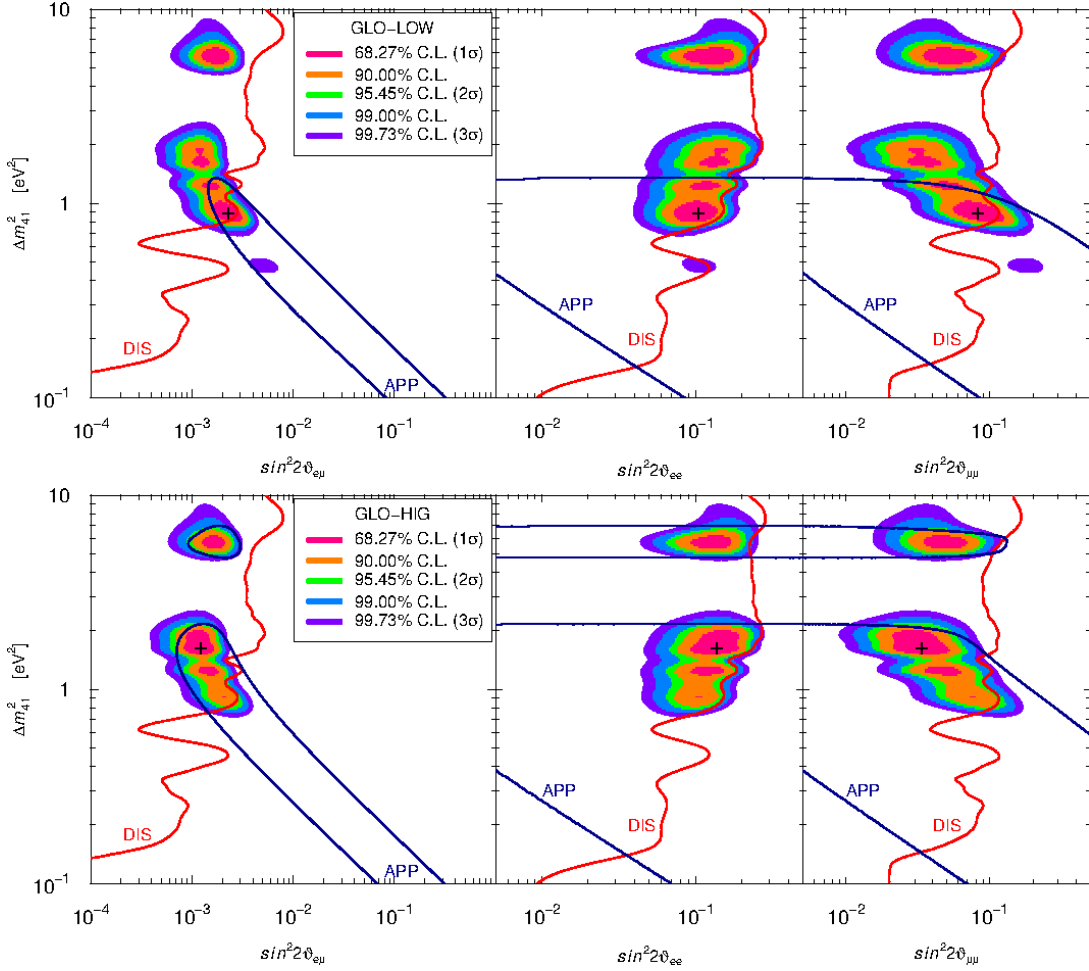


FIG. 3. Allowed regions in the  $\sin^2 2\vartheta_{e\mu} - \Delta m_{41}^2$ ,  $\sin^2 2\vartheta_{ee} - \Delta m_{41}^2$  and  $\sin^2 2\vartheta_{\mu\mu} - \Delta m_{41}^2$  planes obtained from the GLO-LOW and GLO-HIG global analyses of short-baseline neutrino oscillation data (see Tab I). The best-fit points are indicated by crosses (see Table. I). The thick solid blue lines with the label APP show the 3σ allowed regions obtained from the analysis of  $\nu_{\mu} \rightarrow \nu_e$  appearance data. The thick solid red lines with the label DIS show the 3σ allowed regions obtained from the analysis of disappearance data.

fit values of the oscillation parameters listed in Tab. I. The compatibility of the three sets of data is confirmed by the 11% value of the parameter goodness-of-fit [44].

Figure 3 shows the allowed regions in the  $\sin^2 2\vartheta_{e\mu} - \Delta m_{41}^2$ ,  $\sin^2 2\vartheta_{ee} - \Delta m_{41}^2$  and  $\sin^2 2\vartheta_{\mu\mu} - \Delta m_{41}^2$  planes obtained from the global analysis of short-baseline neutrino oscillation data listed in the Introduction. We made two global analyses named GLO-LOW and GLO-HIG, respectively, with and without the three MiniBooNE electron neutrino and antineutrino bins with reconstructed neutrino energy smaller than 475 MeV, which have an excess of events called the “MiniBooNE low-energy anomaly”. The best-fit values of the oscillation parameters are listed in Tab. I. In the global analyses we consider values of  $\Delta m_{41}^2$  smaller than 10 eV<sup>2</sup>, since larger values are strongly incompatible with the cosmological constraints on neutrino masses [33–40].

The GLO-LOW and GLO-HIG analyses are similar,

respectively, to the LOW-GAL and HIG-GAL analyses presented in Ref. [11], but take into account in addition the KARMEN and LSND  $\nu_e - {}^{12}\text{C}$  scattering data. From Fig. 3 and Tab. I one can see that the contribution of the  $\nu_e - {}^{12}\text{C}$  data is beneficial for the lowering of the best-fit value of  $\Delta m_{41}^2$  from 5.6 eV<sup>2</sup> obtained in Ref. [11] to 0.9 eV<sup>2</sup> in GLO-LOW and 1.6 eV<sup>2</sup> in GLO-HIG. These values of  $\Delta m_{41}^2$  are more compatible with the cosmological constraints on neutrino masses [33–40].

Comparing the GLO-LOW and GLO-HIG parts of Fig. 3 and Tab. I one can see that the inclusion of the fit of the MiniBooNE low-energy data favors small values of  $\Delta m_{41}^2$ . This fact has been noted and explained in Ref. [11]. Hence, the results of the GLO-LOW analysis are more attractive than those of the GLO-HIG in view of a better compatibility with cosmological constraints on the neutrino masses.

The well known tension between appearance and disap-

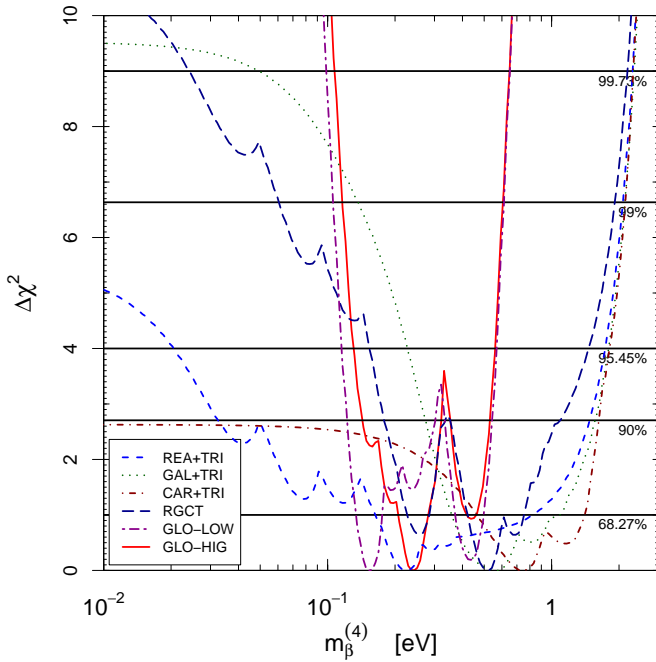


FIG. 4. Marginal  $\Delta\chi^2 = \chi^2 - \chi_{\min}^2$  as a function of the contribution  $m_{\beta}^{(4)} = |U_{e4}|\sqrt{\Delta m_{41}^2}$  to the effective  $\beta$ -decay electron-neutrino mass  $m_{\beta}$  obtained from the fits of Tritium (TRI) data with Reactor (REA), Gallium (GAL) and  $\nu_e$ - $^{12}\text{C}$  (CAR) data, their combined fit (RGCT) and the GLO-LOW and GLO-HIG global fits.

pearance data [11, 19, 59, 61, 73–82] is slightly worsened by the inclusion in the fit of the  $\nu_e$ – $^{12}\text{C}$  scattering data, which strengthen the disappearance constrain.

In the GLO-LOW analysis the 0.008% parameter goodness-of-fit, has worsened with respect to the 0.04% obtained in Ref. [11], which was already so low that we wrote that the MiniBooNE low-energy anomaly “may have an explanation different from  $(\bar{\nu}_{\mu}^-) \rightarrow (\bar{\nu}_e^-)$  oscillations”. Nevertheless, in the following we will discuss the GLO-LOW predictions on the effective neutrino masses measured in  $\beta$ -decay and neutrinoless double- $\beta$ -decay experiments, because we are not aware of an a-priori argument which allows to exclude from the analysis the MiniBooNE low-energy data. The exclusion a-posteriori motivated by the results of the fit may be hazardous, taking also into account the nice value of the global goodness-of-fit (30%) and the above-mentioned preference for small values of  $\Delta m_{41}^2$  in agreement with the same preference of the cosmological data.

Considering the GLO-HIG analysis, the 0.3% appearance-disappearance parameter goodness-of-fit is lower than that obtained in Ref. [11] (1%) because of the above-mentioned strengthening of the disappearance constraint induced by the  $\nu_e$ – $^{12}\text{C}$  scattering data. However, the appearance-disappearance parameter goodness-of-fit is not dramatically low and the fit cannot be rejected, also taking into account the pleasant 50% value

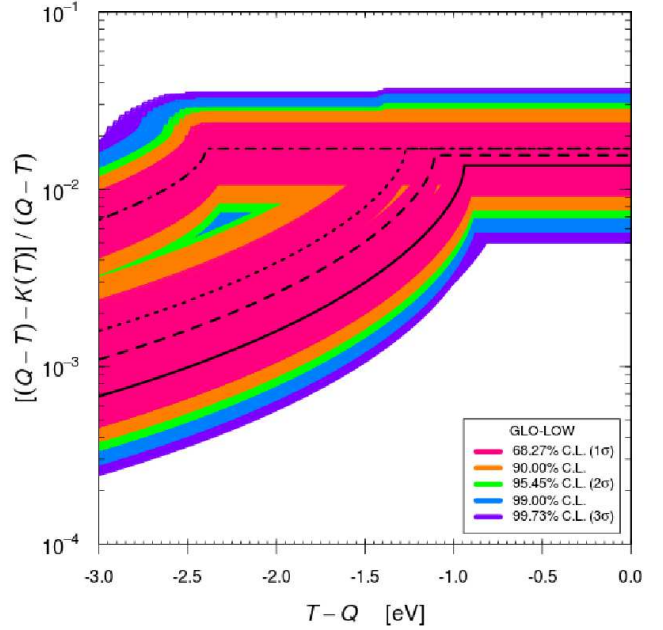


FIG. 5. Bands of the relative deviation of the Kurie plot in  $\beta$ -decay corresponding to the allowed regions in the  $\sin^2 2\vartheta_{ee} - \Delta m_{41}^2$  plane in Fig. 3, obtained from the GLO-LOW global analysis of short-baseline neutrino oscillation data (see Tab I). The black solid line corresponds to the best-fit point ( $m_4 = 0.94$  eV and  $|U_{e4}|^2 = 0.027$ ). The dashed, dotted and dash-dotted lines correspond, respectively, to the local minima at ( $m_4 = 1.11$  eV,  $|U_{e4}|^2 = 0.03$ ), ( $m_4 = 1.27$  eV,  $|U_{e4}|^2 = 0.035$ ) and ( $m_4 = 2.40$  eV,  $|U_{e4}|^2 = 0.033$ ).

of the global goodness-of-fit.

In the next two sections we discuss the predictions for the effective neutrino masses measured in  $\beta$ -decay and neutrinoless double- $\beta$ -decay experiments.

### III. $\beta$ -DECAY

The effective electron neutrino mass  $m_{\beta}$  in  $\beta$ -decay experiments is given by [83–86] (other approaches are discussed in Refs. [87–89])

$$m_{\beta}^2 = \sum_k |U_{ek}|^2 m_k^2. \quad (6)$$

The most accurate measurements of  $m_{\beta}$  have been obtained in the Mainz [90] and Troitsk [91] experiments, whose combined upper bound is [70]

$$m_{\beta} \leq 1.8 \text{ eV} \quad (\text{Mainz+Troitsk, 95\% C.L.}). \quad (7)$$

In the hierarchical 3+1 scheme we have the lower bound

$$m_{\beta} \geq |U_{e4}|\sqrt{\Delta m_{41}^2} \equiv m_{\beta}^{(4)}. \quad (8)$$

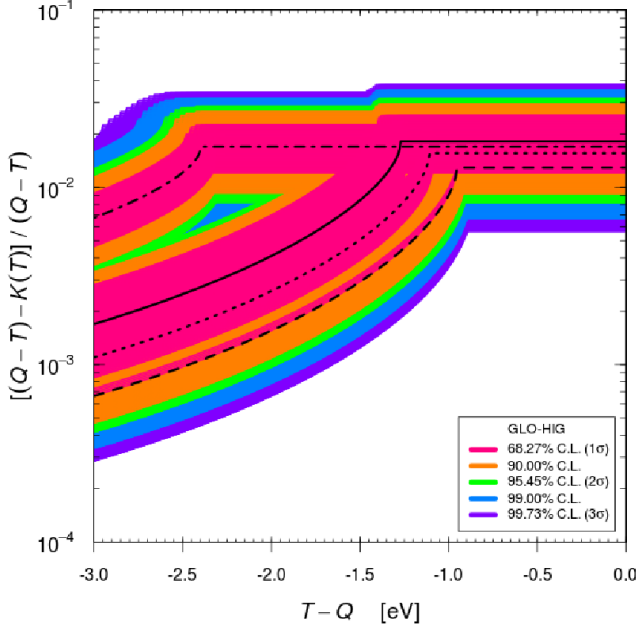


FIG. 6. Bands of the relative deviation of the Kurie plot in  $\beta$ -decay corresponding to the allowed regions in the  $\sin^2 2\vartheta_{ee} - \Delta m_{41}^2$  plane in Fig. 3, obtained from the GLO-HIG global analysis of short-baseline neutrino oscillation data (see Tab I). The black solid line corresponds to the best-fit point ( $m_4 = 1.27$  eV and  $|U_{e4}|^2 = 0.036$ ). The dashed, dotted and dash-dotted lines correspond, respectively, to the local minima at ( $m_4 = 0.95$  eV,  $|U_{e4}|^2 = 0.027$ ), ( $m_4 = 1.11$  eV,  $|U_{e4}|^2 = 0.031$ ) and ( $m_4 = 2.40$  eV,  $|U_{e4}|^2 = 0.033$ ).

Therefore, from the analysis of short-baseline neutrino oscillation data we can derive predictions for the possibility of observing a neutrino mass effect in the KATRIN experiment [92], which is under construction and scheduled to start in 2012, and in other possible future experiments.

Let us however note that the effective electron neutrino mass in Eq. (6) has been derived assuming that all the neutrino masses are smaller than the experimental energy resolution (see Ref. [22]). If  $m_4$  is of the order of 1 eV, the approximation is acceptable for the interpretation of the result of the Mainz and Troitsk experiments, which had, respectively, energy resolutions of 4.8 eV and 3.5 eV [93]. On the other hand, the energy resolution of the KATRIN experiment will be 0.93 eV near the end-point of the energy spectrum of the electron emitted in Tritium decay, at  $T = Q$ , where  $T$  is the kinetic energy of the electron and  $Q = 18.574$  keV is the  $Q$ -value of the decay. If the value of  $m_4$  is larger than the energy resolution of the experiment, its effect on the measured electron spectrum cannot be summarized by one effective

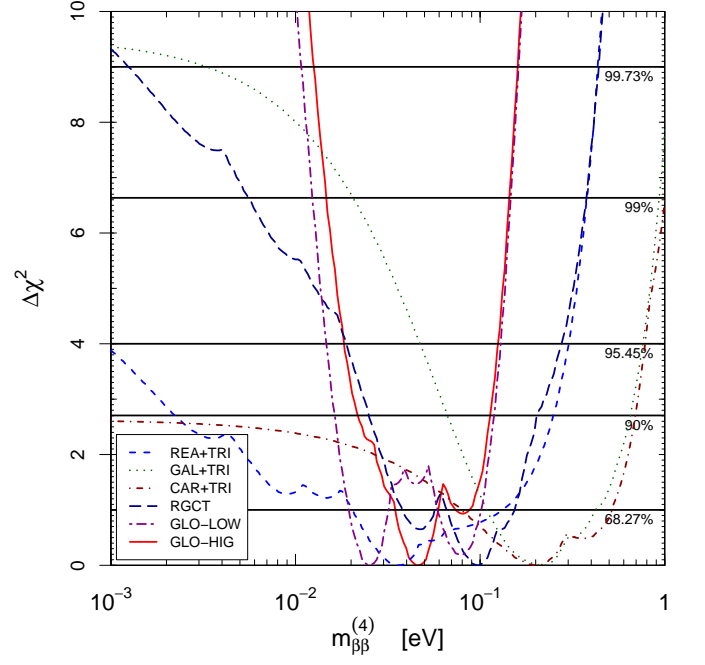


FIG. 7. Marginal  $\Delta\chi^2 = \chi^2 - \chi_{\min}^2$  as a function of the contribution  $m_{\beta\beta}^{(4)} = |U_{e4}|^2 \sqrt{\Delta m_{41}^2}$  to the effective neutrinoless double- $\beta$  decay Majorana mass  $m_{\beta\beta}$  obtained from the fits of Tritium (TRI) data with Reactor (REA), Gallium (GAL) and  $\nu_e$ - $^{12}\text{C}$  (CAR) data, their combined fit (RGCT) and the GLO-LOW and GLO-HIG global fits.

quantity, because the Kurie function  $K(T)$  is given by

$$\frac{K^2(T)}{Q-T} = \sqrt{(Q-T)^2 - \tilde{m}_{\beta}^2} - |U_{e4}|^2(Q-T) + |U_{e4}|^2 \sqrt{(Q-T)^2 - m_4^2} \theta(Q-T-m_4), \quad (9)$$

where  $\tilde{m}_{\beta}^2 = \sum_{k=1}^3 |U_{ek}|^2 m_k^2$  is the contribution of the three neutrino masses much smaller than 1 eV and  $\theta$  is the Heaviside step function.

In the following we discuss the predictions obtained from the GLO-LOW and GLO-HIG analyses of short-baseline neutrino oscillation data for both the contribution  $m_{\beta}^{(4)}$  to the effective mass in  $\beta$ -decay and the distortion of the Kurie function due to  $m_4$ .

Figure 4 shows the marginal  $\Delta\chi^2 = \chi^2 - \chi_{\min}^2$  as a function of  $m_{\beta}^{(4)}$  for the data analyses listed in Tab. II, which gives the 1 $\sigma$ , 2 $\sigma$  and 3 $\sigma$  allowed ranges of  $m_4$ ,  $|U_{e4}|^2$  and  $m_{\beta}^{(4)}$ .

The predictions for  $m_{\beta}^{(4)}$  obtained from the analyses of reactor, Gallium and  $\nu_e - ^{12}\text{C}$  data are interesting, because these data give direct information on  $|U_{e4}|$  from the amplitude of  $\nu_e$  disappearance (see Eq. (5)). Since the data of these experiments do not allow us to constrain the upper value of  $\Delta m_{41}^2$ , as can be seen in Fig. 1, we have analyzed their data in combination with the Tritium data of the Mainz [90] and Troitsk [91] experiment. This is the



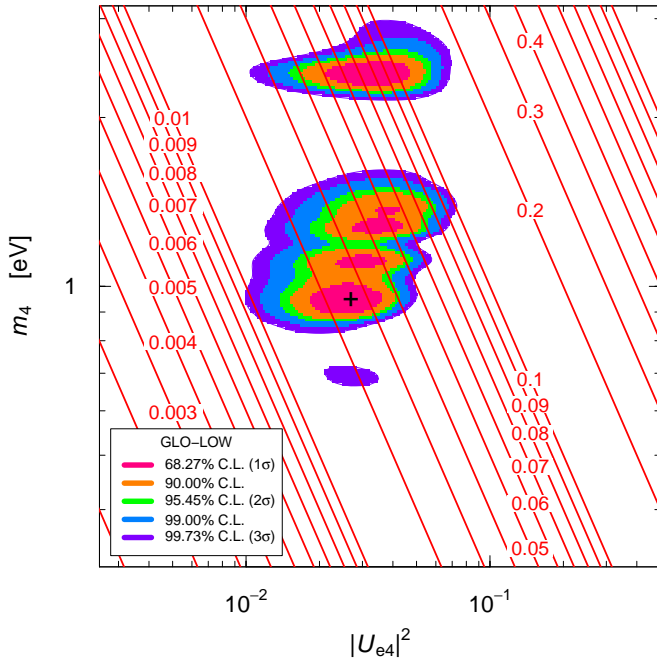


FIG. 8. Allowed regions in the  $|U_{e4}|^2$ - $m_4$  plane obtained from the GLO-LOW global analysis of short-baseline neutrino oscillation data (see Tab I). The best-fit point is indicated by a cross (see Table. I). The red lines have the indicated constant value of  $m_{\beta\beta}^{(4)} = |U_{e4}|^2 \sqrt{\Delta m_{41}^2}$ .

origin of the corresponding upper limits for  $m_4$  and  $m_{\beta}^{(4)}$  in Tab. II and the corresponding steep rise of  $\Delta\chi^2$  for  $m_{\beta}^{(4)} \gtrsim 2$  eV in Fig. 4.

As one can see from Fig. 4 and Tab. II, the most stringent predicted ranges for  $m_{\beta}^{(4)}$  are obtained in the GLO-LOW and GLO-HIG analyses, but all the analyses agree in favoring values of  $m_{\beta}^{(4)}$  between about 0.1 and 0.7 eV, which is promising for the perspectives of future experiments.

In Figures 5 and 6 we show the relative deviation of the Kurie function from the massless case ( $K(T) = Q - T$ ) obtained in the GLO-LOW and GLO-HIG analyses, neglecting the contribution of  $\tilde{m}_{\beta}$  in Eq. (9). For  $T > Q - m_4$  the deviation is constant, because the Kurie function in Eq. (9) reduces to

$$K(T) = (Q - T)\sqrt{1 - |U_{e4}|^2}. \quad (10)$$

For  $T = Q - m_4$  there is a kink and for  $T < Q - m_4$  the Kurie function depends on both  $m_4$  and  $|U_{e4}|^2$ , as given by Eq. (9).

From Figs. 5 and 6 one can see that high precision will be needed in order to see the effect of  $m_4$  and measure  $|U_{e4}|^2$ , which is the only parameter which determines the deviation of  $K(T)$  from the massless Kurie function near the end point, for  $T > Q - m_4$ . If the mixing parameters are near the best-fit point of the GLO-LOW analysis, a precision of about one percent will be needed within

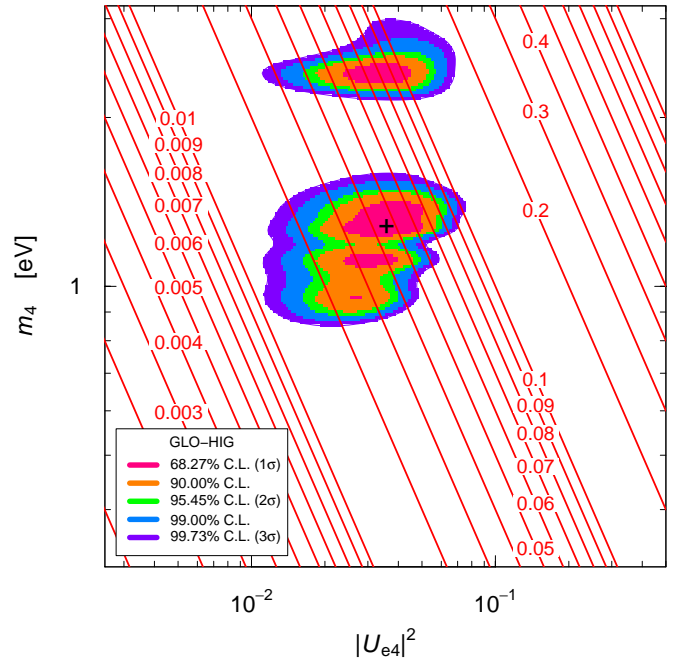


FIG. 9. Allowed regions in the  $|U_{e4}|^2$ - $m_4$  plane obtained from the GLO-HIG global analysis of short-baseline neutrino oscillation data (see Tab I). The best-fit point is indicated by a cross (see Table. I). The red lines have the indicated constant value of  $m_{\beta\beta}^{(4)} = |U_{e4}|^2 \sqrt{\Delta m_{41}^2}$ .

1 eV from the end-point of the spectrum. Finding the effect of  $m_4$  farther from the end-point, for  $T < Q - m_4$  is more difficult, because the relative deviation of the Kurie function can be as small as about  $10^{-3}$ . The GLO-HIG analysis prefers slightly larger values of  $m_4$ , but the discovery of an effect in  $\beta$ -decay will require a similar precision.

#### IV. NEUTRINOLESS $\beta\beta$ -DECAY

If massive neutrinos are Majorana particles, neutrinoless double- $\beta$  decay is possible, with a decay rate proportional to the effective Majorana mass (see Refs. [22, 94–98])

$$m_{\beta\beta} = \left| \sum_k U_{ek}^2 m_k \right|. \quad (11)$$

The results of the analysis of short-baseline oscillation data allow us to calculate the contribution of the heaviest massive neutrino  $\nu_4$  to  $m_{\beta\beta}$ , which is given by

$$m_{\beta\beta}^{(4)} = |U_{e4}|^2 \sqrt{\Delta m_{41}^2}, \quad (12)$$

taking into account the mass hierarchy in Eq. (1). If there are no unlikely cancellations among the contributions of  $m_1$ ,  $m_2$ ,  $m_3$  and that of  $m_4$  [99] (possible cancellations

are discussed in Refs.[100, 101]), the value of  $m_{\beta\beta}^{(4)}$  is a lower bound for the effective neutrino mass which could be observed in future neutrinoless double- $\beta$  decay experiments (see the review in Ref. [102]).

Figure 7 shows the marginal  $\Delta\chi^2$  as a function of  $m_{\beta\beta}^{(4)}$  for the data analyses listed in Tab. II, which gives the  $1\sigma$ ,  $2\sigma$  and  $3\sigma$  allowed ranges of  $m_{\beta\beta}^{(4)}$ .

The analyses of the Gallium and  $\nu_e$ - $^{12}\text{C}$  scattering data give optimistic indications in favor of a value of  $m_{\beta\beta}^{(4)}$  of about 0.2 eV, albeit with large uncertainties, but their combined fit with reactor data lowers the prediction to a best-fit value of about 0.1 eV, with a  $1\sigma$  allowed range which extends down to about 0.04 eV. The reason is that reactor data constrain  $|U_{e4}|^2$  to small values, as can be seen in Tab. II.

The predictions for  $m_{\beta\beta}^{(4)}$  obtained from global GLO-LOW and GLO-HIG agree in indicating a  $3\sigma$  allowed range between about 0.01 and 0.1 eV. The connection of the value of  $m_{\beta\beta}^{(4)}$  with the allowed regions for the oscillation parameters is clarified in Figs. 8 and 9, where we show the allowed regions in the  $|U_{e4}|^2$ - $m_4$  plane obtained, respectively, from the GLO-LOW and GLOW-HIG analyses, together with lines of constant  $m_{\beta\beta}^{(4)}$ . One can see that if the oscillation parameters are close to the best-fit point of the GLO-LOW analysis, at  $m_4 = 0.94$  eV, which is favored by cosmological data, the value of  $m_{\beta\beta}^{(4)}$  is about 0.02-0.03 eV. In order to have a large value of  $m_{\beta\beta}^{(4)}$ , around 0.1 eV, the oscillation parameters must lie in the large- $m_4$  region at  $m_4 \simeq 2.40$  eV, or on the large- $|U_{e4}|^2$  border of the allowed region at  $m_4 \simeq 1.27$  eV.

## V. CONCLUSIONS

In this paper we presented an upgrade of the 3+1 global fit of short-baseline neutrino oscillation data pre-

sented in Ref. [11] obtained with the addition of KARMEN [12, 13] and LSND [14]  $\nu_e + ^{12}\text{C} \rightarrow ^{12}\text{N}_{\text{g.s.}} + e^-$  scattering data, as suggested in Ref. [15]. We have shown that the new data favor low values of  $\Delta m_{41}^2$ , which are appealing in view of the cosmological constraints on neutrino masses [33–40].

We discussed the implications for the measurements of the effective neutrino mass in  $\beta$ -decay and neutrinoless double- $\beta$ -decay experiments.

The predicted contribution of  $m_4$  to the effective neutrino mass  $m_\beta$  in  $\beta$ -decay is in the range between about 0.1 and 0.7 eV, most of which will be explored after 2012 by the KATRIN experiment [92], which will have a sensitivity of about 0.2 eV. If KATRIN or future experiments will have a precision of about one percent near the endpoint of the spectrum, for  $T > Q - m_4$ , the effects of  $m_4$  and  $|U_{e4}|^2$  may be measured separately.

The predicted contribution of  $m_4$  to the effective Majorana mass  $m_{\beta\beta}$  in neutrinoless double- $\beta$  decay is in the range between about 0.01 and 0.1 eV. The expected value of  $m_{\beta\beta}$  is smaller than the expected value of  $m_\beta$  because it is suppressed by an additional power of  $|U_{e4}|$ , which is small. Nevertheless, it is important that  $m_{\beta\beta}$  has a lower limit (if no unlikely cancellations among the four mass contributions occur [99]) which is an important motivation for the development of neutrinoless double- $\beta$  decay experiments [102].

## Acknowledgments

We would like to thank W.C. Louis for interesting discussions.

- 
- [1] LSND, A. Aguilar *et al.*, Phys. Rev. **D64**, 112007 (2001), hep-ex/0104049.
  - [2] MiniBooNE, A. A. Aguilar-Arevalo *et al.*, Phys. Rev. Lett. **105**, 181801 (2010), arXiv:1007.1150.
  - [3] G. Mention *et al.*, Phys. Rev. **D83**, 073006 (2011), arXiv:1101.2755.
  - [4] GALLEX, P. Anselmann *et al.*, Phys. Lett. **B342**, 440 (1995).
  - [5] GALLEX, W. Hampel *et al.*, Phys. Lett. **B420**, 114 (1998).
  - [6] F. Kaether, W. Hampel, G. Heusser, J. Kiko, and T. Kirsten, Phys. Lett. **B685**, 47 (2010), arXiv:1001.2731.
  - [7] SAGE, J. N. Abdurashitov *et al.*, Phys. Rev. Lett. **77**, 4708 (1996).
  - [8] SAGE, J. N. Abdurashitov *et al.*, Phys. Rev. **C59**, 2246 (1999), hep-ph/9803418.
  - [9] SAGE, J. N. Abdurashitov *et al.*, Phys. Rev. **C73**, 045805 (2006), nucl-ex/0512041.
  - [10] SAGE, J. N. Abdurashitov *et al.*, Phys. Rev. **C80**, 015807 (2009), arXiv:0901.2200.
  - [11] C. Giunti and M. Laveder, (2011), arXiv:1109.4033.
  - [12] KARMEN., B. E. Bodmann *et al.*, Phys. Lett. **B332**, 251 (1994).
  - [13] B. Armbruster *et al.*, Phys. Rev. **C57**, 3414 (1998), hep-ex/9801007.
  - [14] LSND, L. B. Auerbach *et al.*, Phys. Rev. **C64**, 065501 (2001), hep-ex/0105068.
  - [15] J. Conrad and M. Shaevitz, (2011), arXiv:1106.5552.
  - [16] Super-Kamiokande, K. Abe *et al.*, Phys. Rev. **D83**, 052010 (2011), arXiv:1010.0118.
  - [17] MINOS, P. Adamson *et al.*, Phys. Rev. Lett. **106**, 181801 (2011), arXiv:1103.0340.
  - [18] S. M. Bilenky, C. Giunti, and W. Grimus, Prog. Part. Nucl. Phys. **43**, 1 (1999), hep-ph/9812360.
  - [19] M. Maltoni, T. Schwetz, M. Tortola, and J. Valle, New



- J. Phys. **6**, 122 (2004), hep-ph/0405172.
- [20] A. Strumia and F. Vissani, (2006), hep-ph/0606054.
  - [21] M. C. Gonzalez-Garcia and M. Maltoni, Phys. Rept. **460**, 1 (2008), arXiv:0704.1800.
  - [22] C. Giunti and C. W. Kim, *Fundamentals of Neutrino Physics and Astrophysics* (Oxford University Press, Oxford, UK, 2007).
  - [23] C. Giunti and Y. Li, Phys. Rev. **D80**, 113007 (2009), arXiv:0910.5856.
  - [24] A. Palazzo, Phys. Rev. **D83**, 113013 (2011), arXiv:1105.1705.
  - [25] S. Choubey, JHEP **12**, 014 (2007), arXiv:0709.1937.
  - [26] S. Razzaque and A. Y. Smirnov, JHEP **07**, 084 (2011), arXiv:1104.1390.
  - [27] R. Gandhi and P. Ghoshal, (2011), arXiv:1108.4360.
  - [28] V. Barger, Y. Gao, and D. Marfatia, (2011), arXiv:1109.5748.
  - [29] G. L. Fogli *et al.*, Phys. Rev. **D78**, 033010 (2008), arXiv:0805.2517.
  - [30] B. A. Reid, L. Verde, R. Jimenez, and O. Mena, JCAP **1001**, 003 (2010), arXiv:0910.0008.
  - [31] S. A. Thomas, F. B. Abdalla, and O. Lahav, Phys. Rev. Lett. **105**, 031301 (2010), arXiv:0911.5291.
  - [32] M. C. Gonzalez-Garcia, M. Maltoni, and J. Salvado, JHEP **08**, 117 (2010), arXiv:1006.3795.
  - [33] J. Hamann, S. Hannestad, G. G. Raffelt, I. Tamborra, and Y. Y. Wong, Phys. Rev. Lett. **105**, 181301 (2010), arXiv:1006.5276.
  - [34] E. Giusarma *et al.*, Phys. Rev. **D83**, 115023 (2011), arXiv:1102.4774.
  - [35] J. R. Kristiansen and O. Elgaroy, (2011), arXiv:1104.0704.
  - [36] Z. Hou, R. Keisler, L. Knox, M. Millea, and C. Reichardt, (2011), arXiv:1104.2333.
  - [37] A. X. Gonzalez-Morales, R. Poltis, B. D. Sherwin, and L. Verde, (2011), arXiv:1106.5052.
  - [38] J. Hamann, S. Hannestad, G. G. Raffelt, and Y. Y. Wong, JCAP **1109**, 034 (2011), arXiv:1108.4136.
  - [39] M. Archidiacono, E. Calabrese, and A. Melchiorri, (2011), arXiv:1109.2767.
  - [40] J. Hamann, (2011), arXiv:1110.4271.
  - [41] R. H. Cyburt, B. D. Fields, K. A. Olive, and E. Skillman, Astropart. Phys. **23**, 313 (2005), astro-ph/0408033.
  - [42] Y. I. Izotov and T. X. Thuan, Astrophys. J. **710**, L67 (2010), arXiv:1001.4440.
  - [43] G. Mangano and P. D. Serpico, Phys. Lett. **B701**, 296 (2011), arXiv:1103.1261.
  - [44] M. Maltoni and T. Schwetz, Phys. Rev. **D68**, 033020 (2003), hep-ph/0304176.
  - [45] KARMEN, B. Armbruster *et al.*, Phys. Rev. **D65**, 112001 (2002), hep-ex/0203021.
  - [46] NOMAD, P. Astier *et al.*, Phys. Lett. **B570**, 19 (2003), hep-ex/0306037.
  - [47] MiniBooNE, A. A. Aguilar-Arevalo, Phys. Rev. Lett. **102**, 101802 (2009), arXiv:0812.2243.
  - [48] MiniBooNE, E. Zimmerman, (2011), PANIC 2011.
  - [49] MiniBooNE, Z. Djurcic, (2011), NUFAC 2011.
  - [50] Bugey, B. Achkar *et al.*, Nucl. Phys. **B434**, 503 (1995).
  - [51] Bugey, Y. Declais *et al.*, Phys. Lett. **B338**, 383 (1994).
  - [52] A. Kuvshinov, L. Mikaelyan, S. Nikolaev, M. Skorkhvatov, and A. Etenko, JETP Lett. **54**, 253 (1991).
  - [53] CalTech-SIN-TUM, G. Zacek *et al.*, Phys. Rev. **D34**, 2621 (1986).
  - [54] A. Hoummada, S. Lazrak Mikou, G. Bagieu, J. Cavaignac, and D. Holm Koang, Applied Radiation and Isotopes **46**, 449 (1995).
  - [55] G. S. Vidyakin *et al.*, Sov. Phys. JETP **71**, 424 (1990).
  - [56] T. A. Mueller *et al.*, Phys. Rev. **C83**, 054615 (2011), arXiv:1101.2663.
  - [57] P. Huber, Phys. Rev. **C84**, 024617 (2011), arXiv:1106.0687.
  - [58] KamLAND, S. Abe *et al.*, Phys. Rev. Lett. **100**, 221803 (2008), arXiv:0801.4589.
  - [59] C. Giunti and M. Laveder, Phys. Rev. **D83**, 053006 (2011), arXiv:1012.0267.
  - [60] CDHSW, F. Dydak *et al.*, Phys. Lett. **B134**, 281 (1984).
  - [61] M. Maltoni and T. Schwetz, Phys. Rev. **D76**, 093005 (2007), arXiv:0705.0107.
  - [62] MINOS, P. Adamson *et al.*, Phys. Rev. Lett. **107**, 011802 (2011), arXiv:1104.3922.
  - [63] D. Hernandez and A. Y. Smirnov, (2011), arXiv:1105.5946.
  - [64] J. N. Bahcall, P. I. Krastev, and E. Lisi, Phys. Lett. **B348**, 121 (1995), hep-ph/9411414.
  - [65] M. Laveder, Nucl. Phys. Proc. Suppl. **168**, 344 (2007), Talk presented at the Workshop on Neutrino Oscillation Physics (NOW 2006), Otranto, Lecce, Italy, 9-16 Sep 2006.
  - [66] C. Giunti and M. Laveder, Mod. Phys. Lett. **A22**, 2499 (2007), hep-ph/0610352.
  - [67] C. Giunti and M. Laveder, Phys. Rev. **D77**, 093002 (2008), arXiv:0707.4593.
  - [68] M. A. Acero, C. Giunti, and M. Laveder, Phys. Rev. **D78**, 073009 (2008), arXiv:0711.4222.
  - [69] C. Giunti and M. Laveder, Phys. Rev. **D80**, 013005 (2009), arXiv:0902.1992.
  - [70] C. Giunti and M. Laveder, Phys. Rev. **D82**, 053005 (2010), arXiv:1005.4599.
  - [71] V. N. Gavrin, V. V. Gorbachev, E. P. Veretenkin, and B. T. Cleveland, (2010), arXiv:1006.2103.
  - [72] C. Giunti and M. Laveder, Phys. Rev. **C83**, 065504 (2011), arXiv:1006.3244.
  - [73] S. M. Bilenky, C. Giunti, and W. Grimus, Eur. Phys. J. **C1**, 247 (1998), hep-ph/9607372.
  - [74] S. M. Bilenky, C. Giunti, W. Grimus, and T. Schwetz, Phys. Rev. **D60**, 073007 (1999), hep-ph/9903454.
  - [75] M. Maltoni, T. Schwetz, M. A. Tortola, and J. W. F. Valle, Nucl. Phys. **B643**, 321 (2002), hep-ph/0207157.
  - [76] M. Sorel, J. Conrad, and M. Shaevitz, Phys. Rev. **D70**, 073004 (2004), hep-ph/0305255.
  - [77] G. Karagiorgi *et al.*, Phys. Rev. **D75**, 013011 (2007), hep-ph/0609177.
  - [78] E. Akhmedov and T. Schwetz, JHEP **10**, 115 (2010), arXiv:1007.4171.
  - [79] G. Karagiorgi, Z. Djurcic, J. Conrad, M. H. Shaevitz, and M. Sorel, Phys. Rev. **D80**, 073001 (2009), arXiv:0906.1997.
  - [80] J. Kopp, M. Maltoni, and T. Schwetz, Phys. Rev. Lett. **107**, 091801 (2011), arXiv:1103.4570.
  - [81] C. Giunti and M. Laveder, (2011), arXiv:1107.1452.
  - [82] G. Karagiorgi, (2011), arXiv:1110.3735, DPF-2011.
  - [83] R. E. Shrock, Phys. Lett. **B96**, 159 (1980).
  - [84] B. H. J. McKellar, Phys. Lett. **B97**, 93 (1980).
  - [85] I. Y. Kobzarev, B. V. Martemyanov, L. B. Okun, and M. G. Shchepkin, Sov. J. Nucl. Phys. **32**, 823 (1980).
  - [86] F. Vissani, Nucl. Phys. Proc. Suppl. **100**, 273 (2001), hep-ph/0012018, Europhysics Neutrino Oscil-

- lation Workshop (NOW 2000), Conca Specchiulla, Otranto, Lecce, Ita, 9–16 Sep 2000.
- [87] Y. Farzan, O. L. G. Peres, and A. Y. Smirnov, Nucl. Phys. **B612**, 59 (2001), hep-ph/0105105.
  - [88] J. Studnik and M. Zralek, (2001), hep-ph/0110232.
  - [89] Y. Farzan and A. Y. Smirnov, Phys. Lett. **B557**, 224 (2003), hep-ph/0211341.
  - [90] C. Kraus *et al.*, Eur. Phys. J. **C40**, 447 (2005), hep-ex/0412056.
  - [91] V. M. Lobashev, Nucl. Phys. **A719**, C153 (2003), 17th International Nuclear Physics Divisional Conference: Europhysics Conference on Nuclear Physics in Astrophysics (NPDC 17), Debrecen, Hungary, 30 Sep – 3 Oct 2002.
  - [92] F. Fraenkle, (2011), arXiv:1110.0087, DPF-2011 Conference, Providence, RI, August 8-13, 2011.
  - [93] C. Weinheimer, (2009), arXiv:0912.1619, International School of Physics 'Enrico Fermi', CLXX course 'Measurements of Neutrino Mass', June 17-27, 2008, Varenna, Italy.
  - [94] S. R. Elliott and P. Vogel, Ann. Rev. Nucl. Part. Sci. **52**, 115 (2002), hep-ph/0202264.
  - [95] S. M. Bilenky, C. Giunti, J. A. Grifols, and E. Masso, Phys. Rep. **379**, 69 (2003), hep-ph/0211462.
  - [96] S. R. Elliott and J. Engel, J. Phys. **G30**, R183 (2004), hep-ph/0405078.
  - [97] I. Avignone, Frank T., S. R. Elliott, and J. Engel, Rev. Mod. Phys. **80**, 481 (2008), arXiv:0708.1033.
  - [98] W. Rodejohann, Int. J. Mod. Phys. **E20**, 1833 (2011), arXiv:1106.1334.
  - [99] C. Giunti, Phys. Rev. **D61**, 036002 (2000), hep-ph/9906275.
  - [100] S. Goswami and W. Rodejohann, Phys. Rev. **D73**, 113003 (2006), hep-ph/0512234.
  - [101] Y. Li and S. shuo Liu, (2011), arXiv:1110.5795.
  - [102] J. Gomez-Cadenas, J. Martin-Albo, M. Mezzetto, F. Monrabal, and M. Sorel, (2011), arXiv:1109.5515.